

An automated archival Very Large Array transients survey

M. E. Bell,^{1*} R. P. Fender,¹ J. Swinbank,² J. C. A. Miller-Jones,^{3,4} C. J. Law,⁵
B. Scheers,^{2,6} H. Spreuw,^{2,7} M. W. Wise,^{2,7} B. W. Stappers,⁸ R. A. M. J. Wijers,²
J. W. T. Hessels^{2,7} and J. Masters³

¹Department of Physics and Astronomy, University of Southampton, University Road, Southampton SO17 1BJ

²Astronomical Institute ‘Anton Pannekoek’, University of Amsterdam, Science Park 904, 1098 XH, Amsterdam, the Netherlands

³NRAO Headquarters, 520 Edgemont Road, Charlottesville, VA 22903, USA

⁴JCRAR – Curtin University of Technology, GPO Box U1987, Perth, WA 6845, Australia

⁵Radio Astronomy Lab, University of California, Berkeley, CA 94720, USA

⁶Centrum Wiskunde and Informatica (CWI), PO Box 94079, 1090 GB, Amsterdam, the Netherlands

⁷Netherlands Institute for Radio Astronomy (ASTRON), Postbus 2, 7990 AA Dwingeloo, the Netherlands

⁸Jodrell Bank Centre for Astrophysics, University of Manchester, Oxford Road, Manchester M13 9PL

Accepted 2011 March 2. Received 2011 February 1; in original form 2010 October 22

ABSTRACT

In this paper we present the results of a survey for radio transients using data obtained from the Very Large Array archive. We have reduced, using a pipeline procedure, 5037 observations of the most common pointings – i.e. the calibrator fields. These fields typically contain a relatively bright point source and are used to calibrate ‘target’ observations: they are therefore rarely imaged themselves. The observations used span a time range ~ 1984 –2008 and consist of eight different pointings, three different frequencies (8.4, 4.8 and 1.4 GHz) and have a total observing time of 435 h. We have searched for transient and variable radio sources within these observations using components from the prototype LOFAR transient detection system. In this paper we present the methodology for reducing large volumes of Very Large Array data; and we also present a brief overview of the prototype LOFAR transient detection algorithms. No radio transients were detected in this survey, therefore we place an upper limit on the snapshot rate of GHz frequency transients > 8.0 mJy to $\rho \leq 0.032 \text{ deg}^{-2}$ that have typical time-scales 4.3 to 45.3 d. We compare and contrast our upper limit with the snapshot rates – derived from either detections or non-detections of transient and variable radio sources – reported in the literature. When compared with the current Log N –Log S distribution formed from previous surveys, we show that our upper limit is consistent with the observed population. Current and future radio transient surveys will hopefully further constrain these statistics, and potentially discover dominant transient source populations. In this paper we also briefly explore the current transient commissioning observations with LOFAR, and the impact they will make on the field.

Key words: astronomical data bases: miscellaneous – radio continuum: general.

1 INTRODUCTION

The scope and depth of transient radio science is vast: by utilizing the time domain we can gain unique insight into such objects as neutron stars and white dwarfs in binary systems, relativistic accretion and consequent jet launch around black holes, distant gamma-ray burst afterglows, supernovae and active galactic nuclei (AGNs), to name a few. The distances to these objects, as well as the time-scale for transient behaviour, varies dramatically. For exam-

ple, giant kilojansky microsecond radio pulses have been observed from the relatively nearby Crab Pulsar (e.g. see Bhat, Tingay & Knight 2008). In contrast, month time-scale (and longer) variations are commonly observed in the radio emission produced by powerful jets driven by accretion on to supermassive black holes in distant AGN (de Vries et al. 2004; Bell et al. 2011; Jones et al. 2011). Through studying the transient and variable nature of these exotic and energetic objects, we obtain an unprecedented laboratory to probe extreme physics.

Despite the scientific potential, the transient and time variable sky is a relatively unexplored region of parameter space. Historically radio transient detections have been sparse due to an inefficient survey

*E-mail: meblw07@soton.ac.uk

figure of merit to adequately sample a large amount of sky to sufficient sensitivity and time resolution (Cordes, Lazio & McLaughlin 2004; Hessels et al. 2009). Some detections of transients have therefore been made serendipitously (e.g. see Davies et al. 1976; Zhao et al. 1992; van den Oord & de Bruyn 1994; Bower et al. 2003 and Lenc et al. 2008). This limitation will soon be relieved by the next generation of wide field telescopes and their respective dedicated transient surveys.

A variety of new wide-field facilities will soon be available to sample the transient sky. In the optical band the Palomar Transient Factory (PTF; Rau et al. 2009) and Panoramic Survey Telescope and Rapid Response System (Pan-STARRS; Hodapp et al. 2004) will survey the sky for transients. In the radio band the Allen Telescope Array (ATA; Welch et al. 2009), the Murchison Wide Field Array (MWA; Lonsdale et al. 2009) and the Low Frequency Array (LOFAR; Fender et al. 2008; Stappers et al. 2011) will soon begin or have already commenced operations. Other wide field radio pathfinders such as the Karoo Array Telescope (MeerKAT; Booth et al. 2009) and the Australian Square-Kilometer-Array Pathfinder (ASKAP; Johnston et al. 2008) are also being developed on the road to the Square Kilometer Array (SKA). Transient studies are a key science goal for all of these facilities.

A common method to detect radio transients is through multi-wavelength triggered observations from, for example, all sky monitors on X-ray observatories. These have produced radio counterparts to gamma-ray burst (GRB) afterglows and black hole X-ray binary outbursts (e.g. see Frail et al. 1997; Eck, Cowan & Branch 2002; Gaensler et al. 2005). This method relies on having a detectable high frequency counterpart, which may be absent (or difficult to detect) for sources such as X-ray dim isolated neutron stars (XDINS; Ofek et al. 2010) and orphan gamma-ray burst afterglows (Frail et al. 1997), demonstrating the need for dedicated radio transient programmes.

Despite the historical challenges, dedicated or commensal transients surveys have produced a number of interesting results. The Galactic Centre (GC) has been the area for some intense observing campaigns; these studies have so far detected a number of radio transients, the most recent being GCRT J1742-3001 (Hyman et al. 2009) and GCRT J1746-2757 (Hyman et al. 2002) – also see Bower et al. (2005). In the high time resolution domain, McLaughlin et al. (2006) discovered short duration transient radio bursts from neutron stars, i.e. Rapidly Rotating Transients (RRATs) – as well as many detections of new pulsars (for example, from the Parkes multibeam Survey).

Nine bursts – named the WJN transients – in excess of 1 Jy have been discovered using drift scan observations with the Waseda Nasu Pulsar Observatory at 1.4 GHz (summarized in Matsumura et al. 2009, but also see Kuniyoshi et al. 2007; Niinuma et al. 2007; Kida et al. 2008; Niinuma et al. 2009 for further details). These are some of the brightest transients reported in the literature and so far remain unexplained. Recently Croft et al. (2010) published results from the ATA Twenty Centimetre Survey (ATATS): no transients were detected and an upper limit on the snapshot rate of events was given. Subsequently the Pi GHz Sky Survey (PiGSS) surveyed the sky with the ATA at 3.1 GHz, providing the deepest static source catalogue to date above 1.4 GHz (Bower et al. 2010). No transients were reported in this survey and an upper limit on snapshot rate was placed.

Searching for highly variable *known* radio sources can also be a useful diagnostic in examining the dynamic radio sky. For example, Carilli, Ivison & Frail (2003) found a number of highly variable ($\Delta S \geq \pm 50$ per cent) radio sources in a small number

of repeated observations of the Lockman Hole at 1.4 GHz. Frail et al. (2003) also found four highly variable radio transient sources from follow-up observations of GRBs at 5 and 8.5 GHz: the rates of these events are consistent with those reported in Carilli et al. (2003). Reporting 39 variable radio sources, Becker et al. (2010) recently characterized the surface density of variables in the direction of the Galactic plane at 4.8 GHz. Most of the variable sources detected had no known multiwavelength counterparts. This is an important study as the rates of transient and variable sources may differ in the direction of Galactic plane when compared with an extra-Galactic pointing. In particular, large numbers of flare stars are known to produce bright coherent bursts (White, Jackson & Kundu 1989), and could dominate detections at low frequencies (Bastian, Dulk & Slee 1988). A deeper discussion on the difference between transient and variable processes will follow later.

Radio telescope archives potentially contain many hours of data which currently remains unsearched for radio transients. An archival study comparing the NRAO Very Large Array (VLA) Sky Survey (NVSS; Condon et al. 1998) and Faint Images of the Radio Sky at Twenty cm (FIRST; Becker, White & Helfand 1995; White et al. 1997) catalogues was conducted by Levinson et al. (2002), with a follow-up study by Gal-Yam et al. (2006): a number of radio transient sources were identified. Bower et al. (2007) analysed 944 epochs of archival VLA data at 4.8 and 8.4 GHz spanning a period of 22 yr. In this survey 10 radio transients were reported, with the host galaxies possibly identified for four out of the 10 sources, and the hosts and progenitors of the other six unknown. Bannister et al. (2011) recently published results from a search for transient and variable sources in the Molonglo Observatory Synthesis Telescope (MOST) archive at 843 MHz. 15 transient and 53 highly variable sources were detected over a 22-yr period. Bannister et al. (2011) use these detections to place limits on the rates of transient and variable sources. Bower & Saul (2011) have published further archival work examining observations of the calibrator 3C286 at 1.4 GHz. A total of 1852 epochs are examined spanning a time range 23 yr: no radio transients were reported.

Bower et al. (2007) with its high yield of transients provided the motivation for this work. The aim of this paper is to push archival radio transient studies further, within the framework of testing and refining the transient detection algorithms that will operate on the LOFAR radio telescope (Fender et al. 2008). We present the findings of an 8.4-, 4.8- and 1.4-GHz study of the repeatedly observed flux and phase-calibrator fields found in the VLA archive. We explore from some of the publications discussed above the reported snapshot rates of either detections of radio transients, or upper limits based on non-detections: we place our own upper limit on these values and discuss the implications.

2 VLA DATA

2.1 VLA calibrator fields

We have searched part of the VLA archive for transients. In order to optimize our chances of success we searched for the most repeatedly observed fields in the VLA archive. The flux and phase calibrator fields were chosen as the backbone of this new transient study. These calibrators are observed routinely and are a standard and necessary calibration technique in radio interferometry. The calibrator fields usually contain a relatively bright compact object, typically a quasar. The calibrators were selected to fulfil one or

Table 1. Number of images reduced and searched with respect to observing frequency. Note, 4.8 and 8.4 GHz were the primary frequencies of interest, 1.4-GHz images were only produced for one field. The calibrators are referred to by their J2000 epoch name. $\langle\delta T_{\text{next}}\rangle$ is the average change in time between sequential observations (including observation on the same day – see Section 2.1). $\langle\tau\rangle$ is the average integration time spent on the calibrator.

Field	RA (J2000)	Dec. (J2000)	ℓ	b	Obs. (8.4 GHz)	# Obs. (4.8 GHz)	# Obs. (1.4 GHz)	$\langle\delta T_{\text{next}}\rangle$ (d)	$\langle\tau\rangle$ (min)
1800+784	18 ^h 00 ^m 45 ^s .7	+78°28 ^m 04 ^s .0	110.0	+29.1	992	908	151	4.3	5.6
0508+845	05 ^h 08 ^m 42 ^s .4	+84°32 ^m 04 ^s .5	128.4	+24.7	205	413	–	13.6	5.1
1927+739	19 ^h 27 ^m 48 ^s .5	+73°58 ^m 01 ^s .6	105.6	+23.5	171	19	–	45.3	9.0
1549+506	15 ^h 49 ^m 17 ^s .5	+50°38 ^m 05 ^s .8	80.2	+49.1	480	558	–	8.3	5.0
0555+398	05 ^h 55 ^m 30 ^s .8	+39°48 ^m 49 ^s .2	171.6	+7.2	123	190	–	27.3	3.5
2355+498	23 ^h 55 ^m 09 ^s .5	+49°50 ^m 08 ^s .3	113.7	–12.0	183	99	–	29.3	7.6/15.3 ^a
3C48	01 ^h 37 ^m 41 ^s .3	+33°09 ^m 35 ^s .1	25.1	+33.4	–	545	–	16.2	4.6
Total					2154	2732	151	1.9/3.0 ^b	5.2

^a7.6 min at 8.4 GHz and 15.3 min at 4.8 GHz.

^b1.9 d including observations on the same day/3.0 d disregarding them.

more of the following criteria: (A) they were observed frequently, (B) they should be unresolved on the longest A-configuration VLA baseline, (C) they had a relatively large integration time per observation. The chosen VLA fields are summarized in Table 1. Note that we initially focused our efforts on the flux calibrators, specifically 3C48; however, with the nature of the bright source in the field and the typically short integration time (~ 1 min) the images often suffered from artifacts. Therefore we quickly switched our attention to the phase calibrators – which proved, due to longer integration times (~ 5 min) to have better image fidelity.

A total of 5037 flux and phase calibrator images have been reduced and searched, with a total observing time of 435 h. The average integration time spent on all sources was $\langle\tau\rangle = 5.2$ min. A full statistical description of the measured noise per image is given in Section 5.

The mean separation between observations regardless of pointing and frequency was $\langle\delta T_{\text{next1}}\rangle = 1.9$ d. When calculating this average we have included observations that occurred on the same day. Note that it is quite common for an observation of the same source to be performed at a number of different frequencies (i.e. sequentially within the same observation). This obviously produces a bias that reduces the average time between observations. When producing the images for this survey we only logged the date of the observations, not the exact start and stop time. Extracting the start and stop time was not easily executed within the imaging pipeline framework. We therefore add in an arbitrary time delay of 4 h in calculating the averages for observations that have the same date. Ignoring observations on the same date yields an average $\langle\delta T_{\text{next2}}\rangle = 3.0$ d (regardless of pointing and frequency).

See the top panel of Fig. 1 for a histogram of the time differences between sequential observations for *all* pointings and frequencies. The bottom panel of Fig. 1 shows a (summed) histogram of the time differences between observations *per pointing*. Table 1 summarizes the average time difference between observations and the average integration time per pointing. The lowest average time difference between observations achieved for one single pointing was 4.3 d (1803+784); the highest was 45.3 d (1927+739). As we have sampled a number of different fields at different cadences we state the range 4.3–45.3 d as the time-scale of transient behaviour that we would be sensitive to. In quoting these numbers we do make the assumption that each image has an equal chance of making a detection – i.e. that there is an isotropic distribution of radio transients and there is no frequency dependence (between 1.4 and 8.4 GHz) for detection.

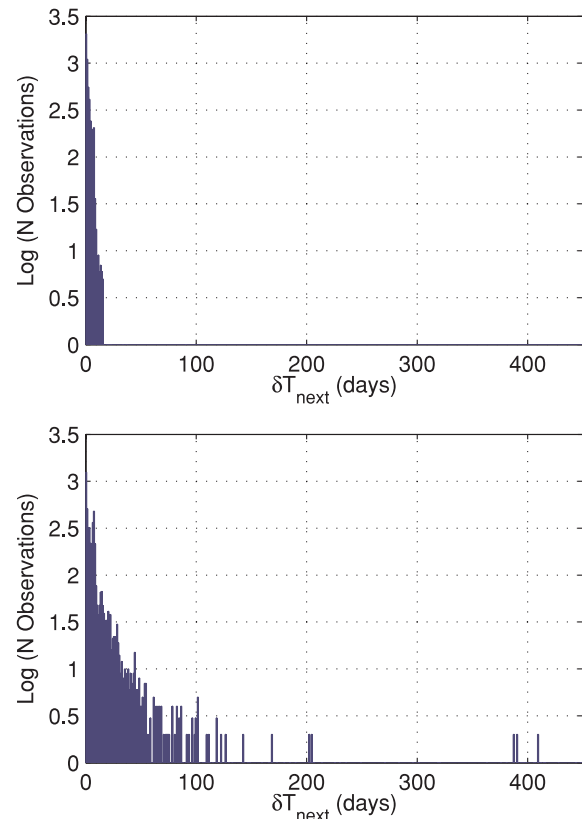


Figure 1. Top Panel: histogram showing the time difference between observations – for *all* pointings and frequencies within this survey. Bottom Panel: a (summed) histogram of the time differences between observations *per pointing* including all frequencies. For a description of the average cadence per pointing see Table 1.

2.2 VLA data analysis

The archival data have been reduced using the ParselTongue (see Kettenis et al. 2006) Python interface to the Astronomical Image Processing System (AIPS; Greisen 2003). A scripted procedure was written to perform the following tasks.

- (i) The data were loaded into AIPS.
- (ii) The antenna table was searched for antennas that were ‘out’ or designated ‘EVLA’ (only relevant 2006 onwards) during the

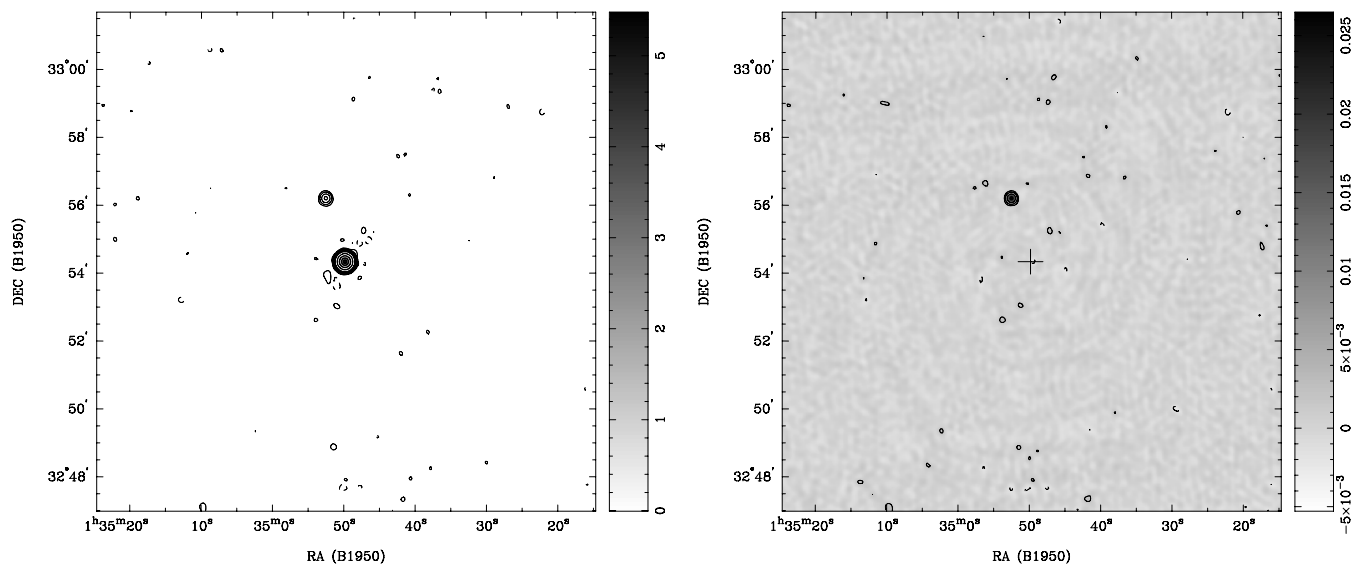


Figure 2. An example image of 3C48 at 4.8 GHz produced by the pipeline (observation date 1984-10-05). The left-hand panel shows a CLEANed image before source subtraction. The right shows the same epoch after source subtraction, a cross denotes the original position of 3C48. The wedge on the right of each image shows the intensity of the Grey-scale in Janskys. The integration time was ~ 4 min, yielding an RMS of 0.6 mJy. Contour levels are $-3, 3, 8, 20, 40, 100, 500, 2000, 5000, 8000 \times \text{RMS}$ for both images.

observations. These antennas were then flagged from being used in subsequent calibration and imaging tasks.

(iii) The maximum baseline length in the observation was ascertained; this was then utilized to optimize cell and image sizes respectively in the subsequent imaging steps.

(iv) The automated flagging procedures were applied to flag unwanted and erroneous visibilities.

(v) The observation log was searched for *any* known flux or phase calibrator¹ used at the VLA within an entire observation.

(vi) For *any* identified calibrator, standard calibration was performed.

(vii) The calibrator was subsequently imaged and deconvolved, followed by three iterations of phase self-calibration only, and then one iteration of amplitude and phase self calibration. The time interval for phase calibration was set appropriately with respect to the integration time on source.

(viii) The calibrator was boxed off, modelled and removed from the image using ultraviolet component subtraction.

(ix) Finally the subtracted image was lightly CLEANed with 150 iterations (Högbom 1974).

The script was designed to be run on large volumes of data without interruption. Python exception handling was used to catch potential errors and remove bad data from further processing. An example image of 3C48 produced by the pipeline before and after source subtraction is shown in Fig. 2. Both images show contours and Grey-scale to give the reader an intuitive feel of the image quality. The source to the North of 3C48 is persistent with a flux ~ 30 mJy and will be discussed further in Section 4.

3 TRANSIENT SEARCH

The images produced by the imaging pipeline were then processed through the prototype LOFAR transient detection algorithms

(Swinbank 2007). By prototype, we refer to a well tested subset of algorithms (taken from LOFAR) that were put together in a ‘pipeline’ to perform the source extraction and databasing for this transient search only. It should be noted that a broader set of algorithms with greater functionality will define the final LOFAR transient detection system.

For each image a background RMS map was calculated over the entire image. For any island of pixels above 8σ i.e. eight times the noise measured from the RMS map, source extraction was performed by fitting elliptical Gaussians. For further details on the LOFAR source extraction algorithms see Spreeuw (2010). In the case of LOFAR images, a subsection of the entire image will be used to calculate a ‘local’ RMS map. Considering the increased field of view of LOFAR, coupled with greater source counts, it is not sufficient to define a global RMS map over the entire image.

A conservative threshold of 8σ was chosen after initial tests and pipeline refinements indicated that a badly calibrated and reduced image – considering the typical strength of the calibrator flux – could produce a large number of artifacts and thus false source detections. All images that were processed by the imaging pipeline were processed through the prototype LOFAR transient detection algorithms – errors included. The rationale for this was to explore the effects of badly calibrated images with respect to source extraction and transient detection. LOFAR will incorporate a false detection rate (FDR) algorithm in the source extraction system, where the global detection threshold for source extraction is set to minimize the number of false positives and is governed by the individual image statistics (Hopkins et al. 2002).

After source extraction a MonetDB (Bonz 2002) data base was then populated with the measured properties and associated data of the extracted sources. The source properties include: position and associated errors, all Stokes parameters of peak and integrated flux including the Gaussian fitting parameters. The associated data included, for example, time of observation, operating frequency and beam properties. The data base was searched for either unique sources that had no previously known counterparts (in previous

¹ Found at <http://www.aoc.nrao.edu/~gtaylor/csource.html>

images), or a known source whose flux had varied by a significant amount. We adopt the same metric used in Carilli et al. (2003) to define significant variability as $\Delta S \geq \pm 50$ per cent.

For further details on the transient data base algorithms, including a mathematical description of the variability measure used in this survey see Scheers (2010). The data base will also cross-reference the transient parameters with those in the Westerbork Northern Sky Survey (WENSS; Rengelink et al. 1997), NVSS and VLA Low-frequency Sky Survey (VLSS; Cohen et al. 2007) catalogues to search for counterparts; for this survey we typically relied on NVSS.

For the majority of fields in this survey, after the calibrator source was subtracted, the fields were left almost devoid of sources: thus the transient search was relatively trivial. A few \sim mJy radio sources were present in some of the fields and only some of the time, due to changing sensitivity. Therefore, we concentrated our efforts on locating unique sources, rather than characterizing the variability of known sources. Once the final list of candidate transient sources had been produced, light curves were automatically generated and the images of interest were checked for calibration errors and image fidelity.

4 RESULTS

A total of 5037 images at various pointings and frequencies have been searched at a detection level of 8σ . Nine candidate transients that were detected in images with adequate image fidelity were scrutinized further. Four of these candidates were found to lie consistently on the dirty beam. After rereduction they were shown to be calibration errors which had been cleaned to a point source.

One candidate was detected 76 times at 4.8 and 8.4 GHz and was found to be significantly variable. After careful consideration and review of the literature it was concluded that this source was created by a bug in the VLA recording system, whereby the pointing of telescopes was changed without updating the header information; this error had affected a previously reported transient VLA J172059.9+385226.6 (see Ofek et al. 2010 for further details). This error was *not* detected in any of the other calibrator images taken around the same time.

Three of the candidates were found to be associated with known weaker radio sources. These sources were detected in the deepest observations (\sim 30 min) of the respective fields. As observations at this depth were very sparse, these radio sources were considered – by the data base algorithms – as transient. These candidates were quickly removed when cross referenced with the radio catalogues. The last transient candidate although surviving some of the rereduction tests was discarded after it was recalibrated and the significance level dropped below adequate levels.

The 3C48 field did contain a persistent source at $\alpha = 01^{\text{h}}37^{\text{m}}44^{\text{s}}.2$ and $\delta = +33^{\circ}11^{\text{m}}26^{\text{s}}.5$ (J2000) with $S_{\nu} \sim 30$ mJy. This source could *not* be identified in the NVSS catalogue, due to insufficient resolution to separate it from 3C48. The FIRST Survey did not cover the position needed to catalogue this source. The source is, however, previously identified in high dynamic range studies of 3C48 (see Briggs 1995). This source was searched for significant variability but none was found.

5 SURFACE DENSITY UPPER LIMIT

As we have detected no radio transients with this survey, we use the area surveyed per observation, coupled with the typical sensitivity

to constrain the snapshot rate of transient events. To calculate the 2σ upper limit of the snapshot rate of transients from our survey we assume a Poisson distribution; for zero detections ($n = 0$) we use

$$P(n) = e^{-\rho N}, \quad (1)$$

where ρ is the snapshot rate of transients; and the 2σ confidence interval is defined as $P(n) = 0.05$ at the 95 per cent confidence level. N is the sum of the number of images multiplied by the field of view (Ω) at that given frequency i.e.

$$N = (\Omega_{8.4} \times N_{8.4}) + (\Omega_{4.8} \times N_{4.8}) + (\Omega_{1.4} \times N_{1.4}). \quad (2)$$

Note, we only consider a search area within the half-power radius per image. Evaluating equations (1) and (2) yields a snapshot rate of $\rho \leq 0.032 \text{ deg}^{-2}$.

To evaluate the flux density limit that we are sensitive to when searching for transients, we must statistically consider the noise measured in all the images. Fig. 3 presents this information in two different ways. First, on the top panel we show a histogram of the measured noise σ_m in all the images; included on the plot is an indicator of the theoretical noise in a 5-min observation (0.16 mJy at 4.8 GHz), and also 10 times this value. Secondly – in the bottom panel – we show a histogram of the measured noise divided by the theoretical noise σ_t (i.e. σ_m/σ_t) for all images: thereby taking into consideration that not all observations were \sim 5 min in duration.

It can be seen that the bulk of the images achieved an image noise less than $10\sigma_t$. Possible deviations away from the theoretical noise could be attributed to, for example, unremoved RFI, bad calibration

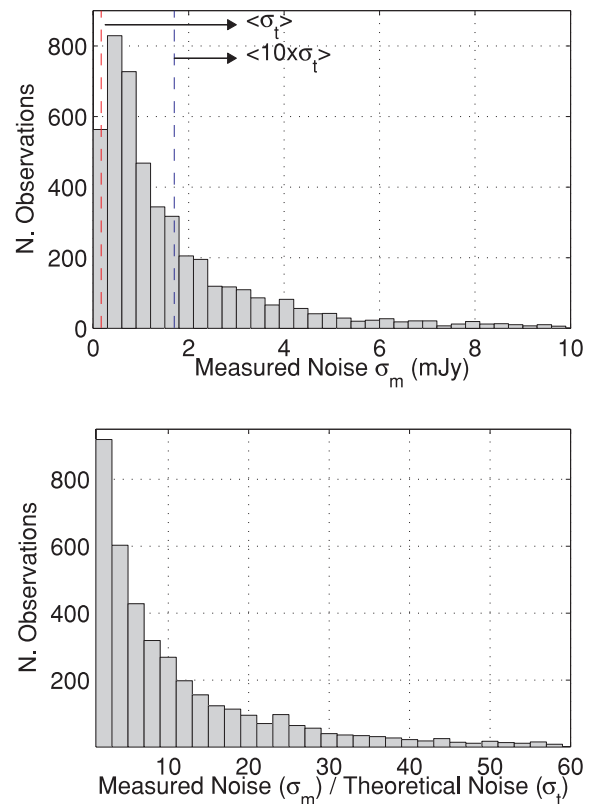


Figure 3. Top panel: histogram showing the measured noise – calculated in the same region – for all images. $\langle \sigma_t \rangle$ gives the theoretical noise calculated from the average integration time for all observations; $\langle 10 \times \sigma_t \rangle$ gives this limit multiplied by 10. Bottom panel: histogram showing the measured noise divided by the theoretical per observation – which accounts for different integration times.

solutions, effects of a bright source in the field and, in general, settings and assumptions within the imaging pipeline that do not lend themselves to a given observation. Taking the median value of all the measured noises we find $\sigma_{\text{median}} = 1 \text{ mJy}$ (or $6.25(\sigma_t)$). Using $8\sigma_{\text{median}}$ as the global detection threshold for the entire survey, we find that we would be sensitive to transients $>8 \text{ mJy}$, with typical time-scales 4.3–45.3 d (see Section 2.1).

In calculating this upper limit we have included *all* images reduced by the pipeline; however, not all images were reduced successfully. Although some images contained artifacts, they rarely contaminated the entire image, thus some area could still be searched effectively. If a unique transient point source was detected in an image with errors, the image was rereduced by hand and checked for reproducibility (see Section 4).

In Fig. 4 we compare the limit imposed on the snapshot rate of sources from this study, with those found in the literature –

this figure is derived from fig. 9 of Bower et al. (2007) and fig. 20 of Croft et al. (2010). We do not include a typical time-scale of the transient duration in the snapshot rate calculation as it is not well constrained. This information is summarized and referenced in Table 2 and described further in the following paragraphs.

The Bower et al. (2007) survey reported the snapshot rate of transients to be $\rho = 1.5 \pm 0.4 \text{ deg}^{-2}$ (labelled ‘B2007^T 1 Week’ in Fig. 4) from eight detections, with characteristic time-scale $20 \text{ min} < t_{\text{char}} < 7 \text{ d}$, above a flux density $370 \mu\text{Jy}$ (with typical image noise $\sim 50 \mu\text{Jy}$ at the pointing centre). Two transients were detected in the 2 month averaged images above a flux density of $200 \mu\text{Jy}$, giving a 2σ limit on the snapshot rate $\rho \sim 2 \text{ deg}^{-2}$ (labelled ‘B2007^T 2 Month’ in Fig. 4). No transients were detected in the year long averages above $90 \mu\text{Jy}$: limiting the 2σ snapshot rate to $\rho < 6 \text{ deg}^{-2}$ (labelled ‘B2007^T 1 Year’ in Fig. 4).

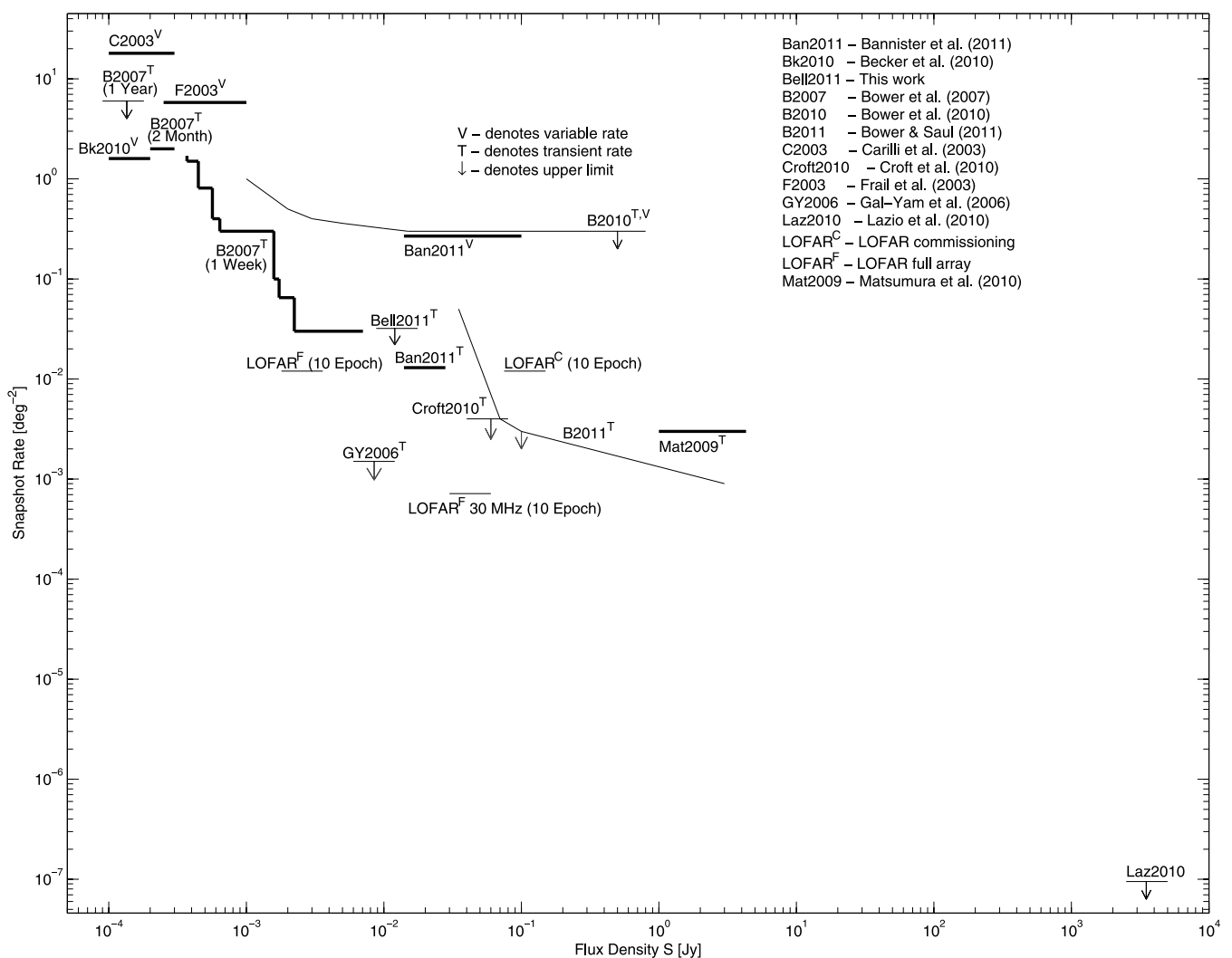


Figure 4. Snapshot rate (deg^{-2}) against flux density (Jy) of detections of transients (labelled ‘T’), detections of variable sources (labelled ‘V’) and upper limits based on non-detections (labelled with downward arrows). The thick black line denotes detections; the thin line denotes upper limits. The Bower et al. (2007) 1-week, 1-yr and 2-month limits are indicated as B2007^T with the appropriate time-scale. Ban2011^V and Ban2011^T indicates the separate rates derived for variables and transients reported in Bannister et al. (2011). Bell2011^T indicates the 2σ upper limits derived from this study. ‘LOFAR^F’ indicates the theoretical constraint that LOFAR could provide with zero detections from 10 epochs of 12 h observations, each of 25 deg^2 fields (using 18 core and 18 remote stations at 150 MHz); ‘LOFAR^C’ indicates the current commissioning capabilities at 150 MHz. ‘LOFAR^F 30 MHz’ shows the rate calculated for a 30 MHz field of view (assuming the final theoretical noise is reached with 18 core and 18 remote stations). We note that this plot does not contain any information on characteristic time duration and recurrence of transient behaviour as both are currently poorly constrained.

Table 2. Summary of snapshot rates reported in the literature. The results are separated out according to upper limits based on non-detections (top), transient detections (middle) and detections of highly variable radio sources (bottom). The flux min column designates the detection threshold of the observations reported in the literature or the minimum flux of detections (indicated as such); the maximum flux is only indicated for transient detections. The Bower et al. (2007) results have been stated three times depending on the characteristic time-scale sampled. We do not give the number of epochs for the WJN transients as it is not stated clearly in the literature. Bower et al. (2010) and Bower & Saul (2011) state two different rates depending on flux density, we quote these separately as (A) and (B).

Survey/Paper	Flux min (μJy)	Flux max (μJy)	ρ (deg^{-2})	t_{char}	ν (GHz)	Epochs (N)
This work	$>8000 (8\sigma)$	–	<0.032	4.3 - 45.3 d	8.4, 4.8 and 1.4	5037
FIRST–NVSS/Gal-Yam et al. (2006)	$>6000^a$	–	$<1.5 \times 10^{-3}$	–	1.4	2^b
ATATS/Croft et al. (2010)	>40000	–	<0.004	81 d – ~ 15 yr	1.4	12^b
Bower et al. (2007)	>90	–	<6	1 yr	4.8 and 8.4	17
PiGSS-I/Bower et al. (2010)(A)	>1000	–	<1	1 month	3.1	75
PiGSS-I/Bower et al. (2010)(B)	>10000	–	<0.3	1 month	3.1	75
Bower & Saul (2011)(A)	>70000	–	$<3 \times 10^{-3}$	1 d	1.4	1852
Bower & Saul (2011)(B)	$>3 \times 10^6$	–	$>9 \times 10^{-4}$	1 d	1.4	1852
Lazio et al. (2010)	$>2.5 \times 10^9 (5\sigma)$	–	$<9.5 \times 10^{-8}$	5 min	0.0738	~ 1272
Bannister et al. (2011)	$14000 (5\sigma)$	6.5×10^6	1.3×10^{-2}	d – yr	0.843	3011^b
Bower et al. (2007)	370	7042	1.5 ± 0.4	20 min – 7 d	4.8 and 8.4	944
Bower et al. (2007)	200	697	2	2 month	4.8 and 8.4	96
WJN/Matsumura et al. (2009)	1×10^6	4.3×10^6	3×10^{-3}	~ 1 d	1.4	–
Bannister et al. (2011)	>14000	–	0.268	day – yr	0.843	3011^b
Carilli et al. (2003)	>100	–	<18	19 d and 17 month	1.4	5
Becker et al. (2010)	>100	–	1.6	~ 15 yr	4.8	3^b
Frail et al. (2003)	>250	–	5.8	~ 1 d	5 and 8.5	–

^aDifferent noise values were found in each survey map thus global threshold taken above 6 mJy.

^bCombined mosaic.

The PiGSS-I Survey using the ATA at 3.1 GHz sets an upper limit on the snapshot rate of transients to $\rho < 1 \text{ deg}^{-2}$ at 1 mJy, and $\rho < 0.3 \text{ deg}^{-2}$ at 10 mJy (labelled ‘B2010^{T,V}’ in Fig. 4), with characteristic time-scale 1 month (Bower et al. 2010). A recent study by Bower & Saul (2011) – using archived VLA observations of the flux calibrator 3C286 at 1.4 GHz – set an upper limit of $\rho < 3 \times 10^{-3} \text{ deg}^{-2}$ at 70 mJy and $\rho < 9 \times 10^{-4} \text{ deg}^{-2}$ at 3 Jy (labelled ‘B2011^T’). The work of Bower & Saul (2011) is very comparable to the work presented in this paper, however, in this study by using predominantly the phase calibrator fields, we slightly push the mean sensitivity down.

The Carilli et al. (2003) study set an upper limit on the rate of highly variable radio sources $\geq 100 \mu\text{Jy}$ to $<18 \text{ deg}^{-2}$ with characteristic time-scales of 19 d and 17 months (labelled ‘C2003^V’ in Fig. 4). Note that these were detections of variable radio sources. Frail et al. (2003) derived a comparable quantity to Carilli et al. (2003) of $\rho \sim 5.8 \text{ deg}^{-2}$ with four highly variable sources with characteristic time-scale ~ 1 d, above a flux density 250 μJy (labelled ‘F2003^V’ in Fig. 4). Similar to these surveys but in the direction of the Galactic plane Becker et al. (2010) found 39 variable radio sources between a flux density range 1–100 mJy, varying on time-scales of years: they derived $\rho \sim 1.6$ Galactic sources deg^{-2} (labelled ‘Bk2010^V’ in Fig. 4).

In the context of this survey, the difference between a variable and a transient – from a purely observational sense – is a matter of detectability; transients sit, most of the time, below the detection capabilities of the instrument, while variables sit above or close to it. However, the underlying astronomical processes associated with transient and variable sources may differ, and should require a different treatment when considering the rates of events. For example, we might expect the rates of variable sources to differ from ‘one off’ explosive transients such as GRB afterglows – which have a finite lifetime and will be undetectable beforehand. For future surveys, a

spectrum of transient and variable behaviour will be observed depending on the cadence and sensitivity. The boundaries between the definitions will become more blurred as the cadence and sensitivity is increased.

The WJN transients summarized in Matsumura et al. (2009) range in flux density from 1 to 4.3 Jy with characteristic time-scale ~ 1 d, yielding a snapshot rate $\rho \sim 3 \times 10^{-3} \text{ deg}^{-2}$ (labelled ‘Mat2009^T’ in Fig. 4). In comparison the Croft et al. (2010) survey set a 2σ upper limit on the snapshot rate of events >40 mJy to be $\rho < 0.004 \text{ deg}^{-2}$; by comparing their source fluxes with those in the NVSS catalogues the characteristic time-scale is ~ 15 yr (labelled ‘Croft2010^T’ in Fig. 4). The most stringent limit placed on the snapshot rate of sources is set by Gal-Yam et al. (2006) to be $\rho < 1.5 \times 10^{-3} \text{ deg}^{-2}$ for flux densities >6 mJy (labelled ‘GY2006^T’ in Fig. 4). Note, the FIRST Survey has improved angular resolution (5arcsec) when compared with NVSS (45arcsec), therefore correct source association effects transient identification. We do not state a characteristic time-scale for the FIRST–NVSS comparison as both individual surveys took a number of years; specific time-scales can only be considered on a source by source basis.

Bannister et al. (2011) set a limit on the snapshot rate of transient sources (calculated from detections) at 0.848 GHz to be $\rho < 1.3 \times 10^{-2} \text{ deg}^{-2}$ above 14 mJy at a variety of time-scales (labelled ‘Ban2011^T’ in Fig. 4). For variable radio sources a rate of $\rho < 0.268 \text{ deg}^{-2}$ is expected between a flux density 14 to 100 mJy (labelled ‘Ban2011^V’ in Fig. 4).

The upper limit derived from this study is consistent with the detections reported by Bower et al. (2007) – we might have expected possibly one detection at our flux density thresholds, assuming that the transient population sampled is isotropically distributed. Bower et al. (2007) did note that an overdensity of galaxies was found within their field. The rate derived from this work is also broadly consistent with that of Bower et al. (2010), Bannister et al. (2011)

and Bower & Saul (2011). If the Bower et al. (2007) and Bannister et al. (2011) detections are of a similar nature, then some of the surveys that report upper limits sit very close to the ‘real’ $\text{Log } N - \text{Log } S$. This is the best benchmark to date to predict the parameter space a given survey should probe to find transients. However, measurements such as frequency dependence and characteristic time-scale of transient behaviour still need to be constrained.

6 PREDICTIONS FOR LOFAR

Commissioning observations are currently underway with LOFAR that are probing the parameter space described in this paper. We include in Fig. 4(a) currently theoretical upper limit of $\rho < 0.012 \text{ deg}^{-2}$ based on zero detections from 10 epochs of 12-h observations, each of 25 deg^2 fields at 150 MHz (labelled LOFAR^C). Early observations with LOFAR around August–September 2010 yield a typical RMS of 15 mJy (75 mJy for a 5σ detection which is plotted) with a bandwidth of 50 MHz spread over 256 subbands (16 channels per subband). However as more baselines have come on-line, and next-generation data reduction strategies have been implemented, improvements upon this value have been made. A more realistic final theoretical noise of 0.36 mJy based on 18 core and 18 remote stations is indicated in Fig. 4 (labelled LOFAR^F). We also include a theoretical prediction based on 10 epochs of 419 deg^2 fields at 30 MHz (labelled ‘LOFAR^F 30 MHz’). This sets an upper limit on the snapshot rate of transients to $\rho < 0.0018 \text{ deg}^{-2}$ above a detection threshold 30 mJy (6 mJy RMS noise).

Recent work by Lazio et al. (2010) using the Long Wavelength Demonstrator Array (LWDA) – a 16 dipole phased array with all-sky imaging capabilities – have performed an all-sky blind transient search. A total of 106 h of data was searched for radio transients at 73.8 MHz – the largest survey yet (in imaging mode) at low frequencies. With no detections of radio transients outside of the solar system above a flux density 500 Jy, an upper limit of $10^{-2} \text{ yr}^{-1} \text{ deg}^{-2}$ is placed on the rate of events. With a typical integration time of 5 min, this converts to $\rho < 9.5 \times 10^{-8} \text{ deg}^{-2}$; we plot this limit in Fig. 4 (labelled ‘Laz2010’) assuming a 5σ (2500 Jy) detection is needed. The Lazio et al. (2010) results tell us that extremely bright radio transients with characteristic time-scale ~ 5 min are very rare. Observations with LOFAR at 30 MHz (see Fig. 4) would be complementary to the Lazio et al. (2010) survey. Approximately 20 tiled pointings could offer the same solid angle coverage as the LWDA i.e. the whole sky, with increased sensitivity. Pushing into this parameter space on a logarithmically spaced range of time-scales (including sub-second parameter space) is a goal for LOFAR, as well as an all-sky monitoring functionality to catch the brightest and rarest exotica.

We can see from Fig. 4 that if LOFAR observations were separated \sim weekly, we would be able – via sampling similar parameter space to the Bower et al. (2007) detections – to test the differences between a GHz and MHz population of radio transients. If the emission mechanism for the GHz population is predominantly via the synchrotron process, then many sources will be initially optically thick within the LOFAR band. The rise time for a distant, luminous, population of radio transients – such as GRB afterglows – could be months or years; with lower peak fluxes. Therefore a steep spectrum population of coherent emitters might dominate detections in the LOFAR band. This coherent population will not be limited by the brightness temperature limit of the synchrotron sources and they could also have more erratic cadences – i.e. switch on and off – which should in turn affect the snapshot rate of events.

Over 10 observations of the same field, with approximately a weekly cadence have already been obtained with LOFAR at 150 MHz. The data reduction is in progress and a concise transient search will follow soon. We therefore hope to test the hypothesis above shortly and push further using future experiments with LOFAR.

7 CONCLUSION

In this paper we have presented the results of an archival VLA study. We have calibrated, imaged and searched 5037 images of the calibrator fields totalling 435 h of observing time. We have presented the methodology for reducing VLA data in a pipeline procedure. We have also explored some of the false detections that can be produced from pipelined image reduction. It should be noted that in general for future surveys our transient detection algorithms should be capable of recognizing (and flagging) common errors associated with interferometric imaging, hence reducing the number of false detections produced. For example, quality control measurements should be included in the pipeline that assess and extract measurements from the observation to remove images from further transient searching.

Even in a very simplistic implementation, these could include, measuring the flux of the calibrator source(s) and removing images where the flux had deviated away from the correct flux, or ignoring any image where more than > 100 sources (or any number more than expected) are extracted. In this survey, a number of candidate transient sources were found to lie on the dirty beam. Source extraction could be performed on the dirty beam and checked for associations in the CLEANed image. Both false and real transient sources can be expected to lie on the dirty beam, however, this information could be used to lower the significance of a given detection in further analysis.

If false detections find their way into the data base, they should be systematically removed to avoid chance source associations in future observations. More complex, and computationally intensive interrogations of the data base should also be performed to find lower significance detections. Greater consideration should also be given to the automated flagging algorithms. For this survey flagged data was very minimal. For LOFAR, however, large amounts of data may be removed, due to the nature of low frequency RFI. Examining the flagged visibilities, or even imaging them, could yield transient detections.

This survey did not detect any radio transients and we have placed a constraint on the snapshot rate of radio transients. We have compared this constraint with results from other surveys, and although we did not detect any transients it is clear that large volumes of parameter space still remain unexplored. As new surveys push into the sub-mJy regime with various cadences and at different frequencies, definitive transient source populations should become apparent. Therefore with the next generation of radio telescopes such as LOFAR becoming available soon, the problem of inadequate sampling of rare transient phenomena will be alleviated. Due also to the triggering of multiwavelength followup the classification and interpretation of these events will come of age.

It seems clear that a large population of bright ($> \text{mJy}$), GHz, frequent events does not exist. Therefore the sub-mJy GHz regime is clearly an important part of parameter space to probe for radio transients. The high dynamic range, and wide-field capabilities, of GHz instruments such as APERTure Tiles In Focus (APERTIF, wide field upgrade to the Westerbork Synthesis Radio Telescope; Verheijen et al. 2008) and ASKAP make them attractive, potentially

high yield, discovery instruments. In summary, a large population of faint (probably distant) transients, as well as very rare bursts remains a strong possibility. Going both deeper and wider with the next generation of radio facilities will allow us to test these possibilities.

ACKNOWLEDGMENTS

The National Radio Astronomy Observatory is a facility of the National Science Foundation operated under cooperative agreement by Associated Universities, Inc. The authors would like to thank the NRAO archive staff for making this work possible. The authors would like to specifically thank John Benson at NRAO archive for delivering vast quantities of archival data. MB would like to thank Bryan Gaensler, Tara Murphy and Keith Bannister from the University of Sydney for their useful comments and discussions. JWTH is a Veni fellow of the Netherlands Foundation for Scientific Research (NWO).

REFERENCES

- Bannister K. W., Murphy T., Gaensler B. M., Hunstead R. W., Chatterjee S., 2011, *MNRAS*, 31
- Bastian T. S., Dulk G. A., Slee O. B., 1988, *AJ*, 95, 794
- Becker R. H., White R. L., Helfand D. J., 1995, *ApJ*, 450, 559
- Becker R. H., Helfand D. J., White R. L., Proctor D. D., 2010, *AJ*, 140, 157
- Bell M. E. et al., 2011, *MNRAS*, 411, 402
- Bhat N. D. R., Tingay S. J., Knight H. S., 2008, *ApJ*, 676, 1200
- Boncz P. A., 2002, PhD thesis, Univ. Amsterdam
- Booth R. S., de Blok W. J. G., Jonas J. L., Fanaroff B., 2009, preprint (arXiv:0910.2935)
- Bower G. C., Saul D., 2011, *ApJ*, 728, L14
- Bower G. C., Plambeck R. L., Bolatto A., McCrady N., Graham J. R., de Pater I., Liu M. C., Baganoff F. K., 2003, *ApJ*, 598, 1140
- Bower G. C., Roberts D. A., Yusef-Zadeh F., Backer D. C., Cotton W. D., Goss W. M., Lang C. C., Lithwick Y., 2005, *ApJ*, 633, 218
- Bower G. C., Saul D., Bloom J. S., Bolatto A., Filippenko A. V., Foley R. J., Perley D., 2007, *ApJ*, 666, 346
- Bower G. C. et al., 2010, *ApJ*, 725, 1792
- Briggs B. S., 1995 PhD thesis, The New Mexico Institute of Mining and Technology
- Carilli C. L., Ivison R. J., Frail D. A., 2003, *ApJ*, 590, 192
- Cohen A. S., Lane W. M., Cotton W. D., Kassim N. E., Lazio T. J. W., Perley R. A., Condon J. J., Erickson W. C., 2007, *AJ*, 134, 1245
- Condon J. J., Cotton W. D., Greisen E. W., Yin Q. F., Perley R. A., Taylor G. B., Broderick J. J., 1998, *AJ*, 115, 1693
- Cordes J. M., Lazio T. J. W., McLaughlin M. A., 2004, *New Astron. Rev.*, 48, 1459
- Croft S. et al., 2010, *ApJ*, 719, 45
- Davies R. D., Walsh D., Browne I. W. A., Edwards M. R., Noble R. G., 1976, *Nat*, 261, 476
- de Vries W. H., Becker R. H., White R. L., Helfand D. J., 2004, *AJ*, 127, 2565
- Eck C. R., Cowan J. J., Branch D., 2002, *ApJ*, 573, 306
- Kuniyoshi M. et al., 2007, *PASP*, 119, 122
- Fender R., Wijers R., Stappers B., LOFAR Transients Key Science Project, 2008, preprint (arXiv:0805.4349)
- Frail D. A., Kulkarni S. R., Nicastro L., Feroci M., Taylor G. B., 1997, *Nat*, 389, 261
- Frail D. A., Kulkarni S. R., Berger E., Wieringa M. H., 2003, *AJ*, 125, 2299
- Gaensler B. M. et al., 2005, *Nat*, 434, 1104
- Gal-Yam A. et al., 2006, *ApJ*, 639, 331
- Greisen E. W., 2003, *Astrophys. Space Sci. Library*, 285, 109
- Hessels J. W. T., Stappers B. W., van Leeuwen J., LOFAR Transients Key Science Project, 2009, preprint (arXiv:0903.1447)
- Hodapp K. W. et al., 2004, *Astron. Nachrichten*, 325, 636
- Högbom J. A., 1974, *A&AS*, 15, 417
- Hopkins A. M., Miller C. J., Connolly A. J., Genovese C., Nichol R. C., Wasserman L., 2002, *AJ*, 123, 1086
- Hyman S. D., Lazio T. J. W., Kassim N. E., Bartleson A. L., 2002, *AJ*, 123, 1497
- Hyman S. D., Wijnands R., Lazio T. J. W., Pal S., Starling R., Kassim N. E., Ray P. S., 2009, *ApJ*, 696, 280
- Johnston S. et al., 2008, *Exp. Astron.*, 22, 151
- Jones S., McHardy I., Moss D., Seymour N., Breedt E., Uttley P., Kording E., Tudose V., 2011, *MNRAS*, 412, 2641
- Kettenis M., van Langevelde H. J., Reynolds C., Cotton B., 2006, *Astron. Data Analysis Software Syst. XV*, 351, 497
- Kida S. et al., 2008, *New Astron.*, 13, 519
- Lazio T. J. W. et al., 2010, *AJ*, 140, 1995
- Lenc E., Garrett M. A., Wucknitz O., Anderson J. M., Tingay S. J., 2008, *ApJ*, 673, 78
- Levinson A., Ofek E. O., Waxman E., Gal-Yam A., 2002, *ApJ*, 576, 923
- Lonsdale C. J. et al., 2009, *Proc. of the IEEE*, 97, 1497
- McLaughlin M. A. et al., 2006, *Nat*, 439, 817
- Matsumura N. et al., 2009, *AJ*, 138, 787
- Niinuma K. et al., 2007, *ApJ*, 657, L37
- Niinuma K. et al., 2009, *ApJ*, 704, 652
- Ofek E. O., Breslauer B., Gal-Yam A., Frail D., Kasliwal M. M., Kulkarni S. R., Waxman E., 2010, *ApJ*, 711, 517
- Rau A. et al., 2009, *PASP*, 121, 1334
- Rengelink R. B., Tang Y., de Bruyn A. G., Miley G. K., Bremer M. N., Roettgering H. J. A., Bremer M. A. R., 1997, *A&A*, 124, 259
- Scheers B., 2010 PhD thesis, Univ. Amsterdam
- Spreeuw J. N., 2010 PhD thesis, Univ. Amsterdam
- Stappers B. W. et al., 2011, preprint (arXiv:1104.1577)
- Swinbank J., 2007, in Tzioumis T., ed., *Proc. Bursts, Pulses and Flickering: Wide-Field Monitoring of the Dynamic Radio Sky*. p. 44
- van den Oord G. H. J., de Bruyn A. G., 1994, *A&A*, 286, 181
- Verheijen M. A. W., Oosterloo T. A., van Cappellen W. A., Bakker L., Ivashina M. V., van der Hulst J. M., 2008, *The Evolution of Galaxies Through the Neutral Hydrogen Window*, 1035, 265
- Welch J. et al., 2009, in Baars J., Thompson R., D'Addario L., eds, *Special Issue of the IEEE, Advances in Radio Telescopes*, in press (arXiv:0904.0762)
- White S. M., Jackson P. D., Kundu M. R., 1989, *ApJS*, 71, 895
- White R. L., Becker R. H., Helfand D. J., Gregg M. D., 1997, *ApJ*, 475, 479
- Zhao J.-H. et al., 1992, *Sci*, 255, 1538

This paper has been typeset from a $\text{\TeX}/\text{\LaTeX}$ file prepared by the author.